Department
of
APPLIED MATHEMATICS

ISSN 0084-778X

Progagation of Shallow Water Inertia-Gravity Waves with Fractional Step Methods

by

Jarle Berntsen and Terje Espelid

Report no. 100 July 1995

Universitetet i Bergen
UNIVERSITY OF BERGEN
Bergen, Norway

Department of Mathematics
University of Bergen
5007 Bergen
Norway

ISSN 0084-778x

Propagation of Shallow Water Inertia-Gravity Waves with Fractional Step Methods

by

Jarle Berntsen and Terje O. Espelid

Report No. 100 July 1995

Propagation of Shallow Water Inertia-Gravity Waves with Fractional Step Methods

Jarle Berntsen
Department of Mathematics
University of Bergen
Johs. Bruns gt. 12
N-5008 Bergen
and
Institute of Marine Research
Nordnesparken 2
N-5024 Bergen

Terje O. Espelid
Department of Informatics
University of Bergen
Thormøhlensgate 55
N-5020 Bergen

Abstract. Fractional step techniques for simulation of ocean circulation are potentially interesting because of their computational simplicity. Several disadvantages with such techniques are however reported. In this paper the propagation of Poincaré Waves in a channel with uniform width and the propagation of the M_2 tide in the North Sea are studied with different fractional step methods and several methods in current use. For these problems symmetrical spatially split fractional step techniques proves to be almost as accurate as implicit methods applied directly on the coupled system of differential equations. Spatially split fractional step methods may as implicit methods be unconditionally stable. This benefit is achieved to a cost which is of the same order of size as for explicit methods.

Subject classification: 65M, 76B

Key words: Shallow water equations, inertia-gravity waves, fractional step methods

1 Introduction.

The CFL-criterion imposed when applying explicit methods in free surface ocean circulation studies, very often forces us to apply smaller time steps than necessary to resolve the major physical processes. This is especially the case when we want to reduce the spatial resolution in areas with large depths. Skagerrak and the Norwegian fjords are examples of such areas.

When applying implicit methods, the CFL-criterion may be avoided or the bound on the time step increased, and the time steps may be chosen according to the time scales of the major processes. On the other hand linear systems of equations have to be solved at each time step and the extra cost of using implicit methods may be significant.

A third approach is to split the system of differential equations in several subsystems of equations. By choosing appropriate numerical techniques for each subsystem the CFL-criterion is affected and may be removed. The cost of solving each sub-problem and also the total cost is often only a small fraction of the cost of applying implicit methods to the complete system of differential equations. The difference equations we get when discretizing the complete system of differential equations may also be split in a similar manner. Combining the two approaches is also possible. All these techniques may be denoted as fractional step methods.

Several disadvantages with fractional step methods due to for instance polarization/one-dimensionalization, need for intermediate boundary conditions and loss of accuracy are reported. Also techniques for avoiding (some of) these problems are suggested. See [4, 6, 9, 13, 14] for further references.

In the present paper the propagation of Poincaré waves in a channel with uniform width and the propagation of the M_2 tide in the North Sea are studied with some potentially interesting fractional step methods.

2 The numerical techniques.

Let f be the Coriolis parameter, g the gravity constant, U and V the depth integrated transports in x and y directions, respectively, η the sea surface elevation and H the undisturbed water depth. The linearized shallow water equations in Cartesian coordinates (x, y) may then be written

$$\begin{aligned} \frac{\partial U}{\partial t} &= -gH\frac{\partial \eta}{\partial x} + fV \\ \frac{\partial V}{\partial t} &= -gH\frac{\partial \eta}{\partial y} - fU \\ \frac{\partial \eta}{\partial t} &= -\frac{\partial U}{\partial x} - \frac{\partial V}{\partial y}. \end{aligned} \tag{1}$$

The quality of different numerical methods for computing approximate solutions to (1) will be studied. The variables are approximated in an Arakawa C-grid, see Fig. 1. H too is known in the η points. The same spatial discretization is applied for all time stepping techniques

$$\begin{aligned}
\frac{\partial U_{ij}}{\partial t} &\sim -g(\mu_x H_{ij})\delta_x \eta_{ij} + f\mu_{xy} V_{ij} \\
\frac{\partial V_{ij}}{\partial t} &\sim -g(\mu_y H_{ij})\delta_y \eta_{ij} - f\mu_{xy} U_{ij} \qquad (2) \\
\frac{\partial \eta_{ij}}{\partial t} &\sim -\delta_x U_{ij} - \delta_y V_{ij}.
\end{aligned}$$

where

$$\begin{aligned}
\mu_x F(x,y) &= (F(x+\Delta x/2, y) + F(x-\Delta x/2, y))/2 \\
\delta_x F(x,y) &= (F(x+\Delta x/2, y) - F(x-\Delta x/2, y))/\Delta x \\
\mu_{xy} F(x,y) &= (F(x+\Delta x/2, y+\Delta y/2) + F(x+\Delta x/2, y-\Delta y/2) + \\
&\quad F(x-\Delta x/2, y-\Delta y/2) + F(x-\Delta x/2, y+\Delta y/2))/4.
\end{aligned}$$

Δx is the grid size in the x-direction. The grid size in y-direction, Δy, will be equal to Δx in all our experiments. The remaining averaging and difference operations in (2) are defined correspondingly. Different techniques for stepping the numerical approximations forward in time are considered.

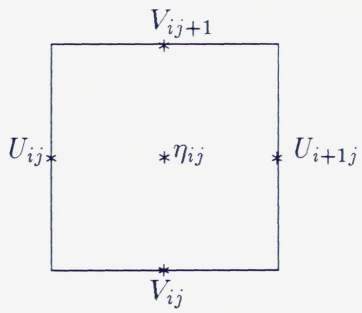

Fig. 1 The variables in an Arakawa C-grid.

2.1 The forward-backward scheme.

$$\begin{aligned}
\eta_{ij}^{n+1} &= \eta_{ij}^{n} - \Delta t(\delta_x U_{ij}^{n} + \delta_y V_{ij}^{n}) \\
U_{ij}^{n+1} &= U_{ij}^{n} - \Delta t(g(\mu_x H_{ij})\delta_x \eta_{ij}^{n+1} - f\mu_{xy} V_{ij}^{n}) \\
V_{ij}^{n+1} &= V_{ij}^{n} - \Delta t(g(\mu_y H_{ij})\delta_y \eta_{ij}^{n+1} + f\mu_{xy} U_{ij}^{n+1}).
\end{aligned}$$

This is a much referenced explicit scheme, see for instance Haltiner and Williams [8] and Beckers and Deleersnijder [3]. We note that the treatment of the Coriolis term is explicit in the U-equation and implicit in the V-equation. In the next time step the V-equation is treated before the U-equation and the Coriolis terms are then treated explicitly in the V-equation and implicitly in the U-equation. For gravity waves this scheme is stable as long as the time step Δt satisfies the CFL-criterion $\Delta t < \Delta x/\sqrt{2gH}$.

2.2 The Crank-Nicolson method.

The method due to Crank and Nicolson [5] applied to our system of equations may be written

$$U_{ij}^{n+1} = U_{ij}^{n} - \frac{\Delta t}{2}(g(\mu_x H_{ij})\delta_x(\eta_{ij}^{n+1} + \eta_{ij}^{n}) - f\mu_{xy}(V_{ij}^{n+1} + V_{ij}^{n})) \tag{3}$$

$$V_{ij}^{n+1} = V_{ij}^{n} - \frac{\Delta t}{2}(g(\mu_y H_{ij})\delta_y(\eta_{ij}^{n+1} + \eta_{ij}^{n}) + f\mu_{xy}(U_{ij}^{n+1} + U_{ij}^{n})) \tag{4}$$

$$\eta_{ij}^{n+1} = \eta_{ij}^{n} - \frac{\Delta t}{2}(\delta_x(U_{ij}^{n+1} + U_{ij}^{n}) + \delta_y(V_{ij}^{n+1} + V_{ij}^{n})). \tag{5}$$

This method is 2nd order accurate in time and space and unconditionally stable. When computing the solution at time step $n+1$, we may follow Backhaus [1] and insert (3) and (4) into (5) to find that η_{ij}^{n+1} depends on unknowns in 13 grid points. The three equations above will still be coupled with this insertion.

2.3 Inertia-Gravity splittings.

The linearized shallow water equations (1) may be split into two sub-systems of differential equations

$$\begin{aligned}
\frac{\partial U}{\partial t} &= fV \\
\frac{\partial V}{\partial t} &= -fU \\
\frac{\partial \eta}{\partial t} &= 0
\end{aligned} \tag{6}$$

and

$$\begin{aligned} \frac{\partial U}{\partial t} &= -gH\frac{\partial \eta}{\partial x} \\ \frac{\partial V}{\partial t} &= -gH\frac{\partial \eta}{\partial y} \\ \frac{\partial \eta}{\partial t} &= -\frac{\partial U}{\partial x} - \frac{\partial V}{\partial y}. \end{aligned} \tag{7}$$

The first sub-system (6) is a coupled system of two ordinary differential equations which may, for given initial values, be solved exactly if U and V were defined in the same points in space. For the C-grid the solution of (6) is approximated by

$$U_{ij}^{n*} = \alpha U_{ij}^{n} + \beta \mu_{xy} V_{ij}^{n} \tag{8}$$

$$V_{ij}^{n*} = \alpha V_{ij}^{n} - \beta \mu_{xy} U_{ij}^{n} \tag{9}$$

where $\alpha = cos(f\Delta t)$, $\beta = sin(f\Delta t)$ and the superscript $n*$ (instead of $n+1$) indicates that this is only an intermediate solution. The Crank-Nicolson method applied to sub-system (7) of equations may be written

$$U_{ij}^{n*} = U_{ij}^{n} - \frac{\Delta t}{2} g(\mu_x H_{ij})\delta_x(\eta_{ij}^{n*} + \eta_{ij}^{n}) \tag{10}$$

$$V_{ij}^{n*} = V_{ij}^{n} - \frac{\Delta t}{2} g(\mu_y H_{ij})\delta_y(\eta_{ij}^{n*} + \eta_{ij}^{n}) \tag{11}$$

$$\eta_{ij}^{n*} = \eta_{ij}^{n} - \frac{\Delta t}{2}(\delta_x(U_{ij}^{n*} + U_{ij}^{n}) + \delta_y(V_{ij}^{n*} + V_{ij}^{n})). \tag{12}$$

Here too we may insert (10) and (11) into (12) when solving for η_{ij}^{n*}. Using the notation

$$\begin{aligned} \gamma_x &= \Delta t g(\mu_x H_{ij})\delta_x/2 \\ \gamma_y &= \Delta t g(\mu_y H_{ij})\delta_y/2 \\ \lambda_x &= g(\Delta t)^2\delta_x(\mu_x H_{ij})\delta_x/4 \\ \lambda_y &= g(\Delta t)^2\delta_y(\mu_y H_{ij})\delta_y/4 \end{aligned}$$

we may, after insertion of (10) and (11) into (12), write

$$U_{ij}^{n*} = U_{ij}^{n} - \gamma_x(\eta_{ij}^{n*} + \eta_{ij}^{n}) \tag{13}$$

$$V_{ij}^{n*} = V_{ij}^{n} - \gamma_y(\eta_{ij}^{n*} + \eta_{ij}^{n}) \tag{14}$$

$$\eta_{ij}^{n*} = \eta_{ij}^{n} - \Delta t(\delta_x U_{ij}^{n} + \delta_y V_{ij}^{n}) + (\lambda_x + \lambda_y)(\eta_{ij}^{n*} + \eta_{ij}^{n}). \tag{15}$$

We note that η_{ij}^{n*} is decoupled from U and V at intermediate time step $n*$ and involves 5 unknowns at time step $n*$. The computational complexity is therefore considerably reduced by introducing the suggested splitting. The quality of the model results may however be reduced also and will depend on the order in which the systems (6) and (7) are solved. Introducing

$$W_{ij} = \begin{pmatrix} U_{ij} \\ V_{ij} \\ \eta_{ij} \end{pmatrix}$$

(8) and (9) may be written

$$W_{ij}^{n*} = CW_{ij}^{n}$$

where the operator C is given by

$$C = \begin{pmatrix} \alpha & \beta\mu_{xy} & 0 \\ -\beta\mu_{xy} & \alpha & 0 \\ 0 & 0 & 1 \end{pmatrix}.$$

(13), (14) and (15) may be written

$$\begin{pmatrix} 1 & 0 & \gamma_x \\ 0 & 1 & \gamma_y \\ 0 & 0 & 1-\lambda_x-\lambda_y \end{pmatrix} W_{ij}^{n*} = \begin{pmatrix} 1 & 0 & -\gamma_x \\ 0 & 1 & -\gamma_y \\ -\Delta t\delta_x & -\Delta t\delta_y & 1+\lambda_x+\lambda_y \end{pmatrix} W_{ij}^{n}$$

or formally

$$W_{ij}^{n*} = GW_{ij}^{n}. \tag{16}$$

The operations may then be combined in different ways to compute values at time step $n+1$

Alternative 1: $W_{ij}^{n+1} = GCW_{ij}^{n}$.

Alternative 2: $W_{ij}^{n+1} = CGW_{ij}^{n}$.

The operations may also be symmetrized over a double step

Alternative 3: $W_{ij}^{n+2} = CGGCW_{ij}^{n}$.

Since the two operators G and C do not commute only the third alternative will be 2nd order in time regarded over a double step, see Strang [12].

2.4 Spatial splitting of the gravity difference equations.

Even if the splitting introduced above reduces the computational complexity considerably, the cost of solving the linear system (16) will be significant and for iterative techniques the cost will depend on the size of the off-diagonal elements, that is Δt and H. As indicated above we first solve for η_{ij}^{n*} and then for U_{ij}^{n*} and V_{ij}^{n*} when performing the operations (16). We may apply a Douglas-Rachford type alternating direction implicit technique, see Weiyan [14] p. 367, to split the G operator spatially, and the following sequence of operations may get us from time step n to time step $n+1$.

1. The Coriolis terms. $W_{ij}^{n*} = CW_{ij}^{n}$.

2. Implicit split in x-direction.

$$\begin{pmatrix} 1 & 0 & 0 \\ 0 & 1 & 0 \\ 0 & 0 & 1-\lambda_x \end{pmatrix} W_{ij}^{n**} = \begin{pmatrix} 1 & 0 & -\gamma_x \\ 0 & 1 & -\gamma_y \\ -\Delta t\delta_x & -\Delta t\delta_y & 1+\lambda_x+2\lambda_y \end{pmatrix} W_{ij}^{n*}.$$

3. Implicit split in y-direction.

$$\begin{pmatrix} 1 & 0 & 0 \\ 0 & 1 & 0 \\ 0 & 0 & 1-\lambda_y \end{pmatrix} W_{ij}^{n***} = W_{ij}^{n**} + \begin{pmatrix} 0 & 0 & 0 \\ 0 & 0 & 0 \\ 0 & 0 & -\lambda_y \end{pmatrix} W_{ij}^{n*}.$$

4. Solve for U and V.

$$\begin{pmatrix} 1 & 0 & \gamma_x \\ 0 & 1 & \gamma_y \\ 0 & 0 & 1 \end{pmatrix} W_{ij}^{n+1} = W_{ij}^{n***}.$$

The steps 1 to 4 may formally be written

$$W_{ij}^{n+1} = G_{xy}CW_{ij}^{n}.$$

The Coriolis terms may be treated in the final substep

$$W_{ij}^{n+1} = CG_{xy}W_{ij}^{n}$$

or we may symmetrize the operations over a double step

$$W_{ij}^{n+2} = CG_{xy}G_{xy}CW_{ij}^{n}. \tag{17}$$

We may also step implicitly in y-direction before taking an implicit step in x-direction. Such a procedure may formally be written

$$W_{ij}^{n+1} = G_{yx}CW_{ij}^{n}$$

The procedure (17) will be 2nd order both in time and space regarded over a double step. In order to reduce the effect of polarization, it may be useful to symmetrize the order in which the directions are treated

$$W_{ij}^{n+2} = CG_{yx}G_{xy}CW_{ij}^{n}.$$

Replacing G by G_{xy} or G_{yx}, we get two three-diagonal systems of equations to solve at each time step. This means a considerable simplification in computational complexity. On the other hand this splitting may result in stability problems and loss of accuracy.

2.5 Spatial splitting of the gravity differential equations.

Instead of splitting the discrete operator G spatially, the subsystem (7) of differential equations may be split in two new subsystems

$$\begin{aligned} \frac{\partial U}{\partial t} &= -gH\frac{\partial \eta}{\partial x} \\ \frac{\partial V}{\partial t} &= 0 \\ \frac{\partial \eta}{\partial t} &= -\frac{\partial U}{\partial x} \end{aligned} \tag{18}$$

and

$$\begin{aligned} \frac{\partial U}{\partial t} &= 0 \\ \frac{\partial V}{\partial t} &= -gH\frac{\partial \eta}{\partial y} \\ \frac{\partial \eta}{\partial t} &= -\frac{\partial V}{\partial y}. \end{aligned} \tag{19}$$

Each subsystem is one-dimensional and may be propagated in time with the Crank-Nicolson method. The following sequence of operations may get us from time step n to time step $n+1$.

1. The Coriolis terms. $W_{ij}^{n*} = CW_{ij}^{n}$.

2. Crank-Nicolson on subsystem (18).

$$\begin{pmatrix} 1 & 0 & \gamma_x \\ 0 & 1 & 0 \\ 0 & 0 & 1-\lambda_x \end{pmatrix} W_{ij}^{n**} = \begin{pmatrix} 1 & 0 & -\gamma_x \\ 0 & 1 & 0 \\ 0 & 0 & 1+\lambda_x \end{pmatrix} W_{ij}^{n*}. \tag{20}$$

3. Crank-Nicolson on subsystem (19).

$$\begin{pmatrix} 1 & 0 & 0 \\ 0 & 1 & \gamma_y \\ 0 & 0 & 1-\lambda_y \end{pmatrix} W_{ij}^{n+1} = \begin{pmatrix} 1 & 0 & 0 \\ 0 & 1 & -\gamma_y \\ 0 & 0 & 1+\lambda_y \end{pmatrix} W_{ij}^{n**}. \tag{21}$$

The steps 1 to 3 may formally be written

$$W_{ij}^{n+1} = G_y G_x C W_{ij}^{n}.$$

As for the previous splitting technique the order of the operations may be reversed or symmetrized over a double step.

According to von Neumann stability analysis for free waves all methods above, except for the forward-backward method, are unconditionally stable. For waves in regions with varying topography and/or non-straight coasts, the eigenvalues of the corresponding propagation matrices must be studied before any firm conclusions with respect to stability can be drawn.

Intermediate boundary conditions are a problem when applying fractional step methods. With all variables defined in the same points (A-grid) and non-rectangular regions, it is especially difficult to define intermediate boundary conditions when applying ADI type techniques. With the C-grid $U = 0$ or $V = 0$ in land/sea points and the η-points closest to land cells become decoupled from boundary points.

When applying non-spatial split implicit methods, the solutions of the corresponding linear systems of equations are iterated to machine accuracy using the Gauss-Seidel iterative technique.

3 Poincaré Waves.

In Gill [7] it is shown how waves in a channel of uniform width, W, and uniform depth, H, may be combined to form a solution of our system of equations (1). The solution is

$$\begin{aligned} \eta(x,y,t) &= \left(\frac{2\eta_0}{\kappa\omega_c}\right)(kfcos(ly)+\omega lsin(ly))cos(kx-\omega t) \\ U(x,y,t) &= \left(\frac{2gH\eta_0}{\kappa\omega_c}\right)(klsin(ly)+(\omega f/gH)cos(ly))cos(kx-\omega t) \quad (22) \\ V(x,y,t) &= \left(\frac{2\omega_c\eta_0}{\kappa}\right)cos(ly)sin(kx-\omega t) \end{aligned}$$

where η_0 is the amplitude, ω the frequency, $\mathbf{k} = (k,l)$ the wavenumber, $\kappa = \sqrt{k^2+l^2}$ the magnitude of the wavenumber, $\omega_c = \sqrt{f^2+l^2gH}$ and $\omega = \sqrt{\omega_c^2+k^2gH}$. In addition l must satisfy

$$l = n_y\pi/W, \quad n_y = 1,3,5,....$$

We also choose k such that

$$k = n_x\pi/L, \quad n_x = 1,2,3,....$$

where L is the length of the channel. Numerical approximations to η will be compared with the analytical solution (22) and Table 1 shows the physical parameters used in our experiments. The channel is placed such that the corner points are $(0,-W/2),(L,-W/2),(0,W/2)$ and $(L,W/2)$ in the (x,y) plane. The channel is discretized in a $20*20$km Arakawa C-grid giving 150*30 horizontal grid cells within the channel. At the inflow boundary $(0,y), -W/2 \leq y \leq W/2$ analytical values of U,V and η are used to define boundary values. At the outflow boundary a FRS-zone, see Martinsen and Engedahl [10], is added to the computational domain. In the 10 cell wide zone the numerical approximations are "relaxed" towards the analytical values. The boundaries $(x,-W/2), 0 \leq x \leq L$ and $(x,W/2), 0 \leq x \leq L$ are closed ($V = 0$).

The analytical values of η, U and V at time $t = 0$ are used as initial values in all grid points. For gravity waves the CFL-criterion for the forward-backward method is $\Delta t < \Delta x/\sqrt{2gH} = 451.52$. We want to relate our time steps to this criterion. To be able to compute statistics over periods in time, integer numbers of steps over a period, $2\pi/\omega$, are applied. The waves need approximately 39 hours to travel the distance L, and in all experiments the waves are simulated 50 hours. In Table 2 the maximum errors in the numerical approximations to η

(maximum in space and time) produced by the different methods are compared. The operator splitting methods applied are defined in the previous section and identified through their propagation operators. Results for a method applied by Backhaus [2] are also reported. In this method the Coriolis terms are treated exactly without separating them from the pressure terms. The linear system of equations is iterated to solve the remaining implicit problem. We note that for small time steps the errors are similar for all methods. This is as expected because the same spatial discretizations are applied and for small Δt the spatial errors dominate. For $\Delta t = 437$s the maximum error for the forward-backward technique is somewhat larger than for many of the other techniques, but taking the computational simplicity into account it competes favorably. For larger time steps the qualities of the model results measured in this norm are also similar for all methods except for the forward-backward method. Therefore, we conclude that the spatial splitting techniques compete very favorably with the more implicit techniques on this problem. From the table we see that to symmetrize the propagation matrices over a double step does not result in obvious improvements in the approximations to η. We also note that all the splitting techniques compete favorably with the method applied by Backhaus.

In some cases we are not primarily interested in these waves themselves, but in their influence on the mean circulation. For the solution (22) average time integrated values are

$$\overline{\phi} = \frac{\omega}{2\pi} \int_0^{\frac{2\pi}{\omega}} \phi dt = 0 \tag{23}$$

for $\phi = U, V$ or η. The numerical solution should also satisfy the condition of no net flow over a period.

In the figures 2 to 6 the spatial distribution of approximations to $\overline{U}$ are plotted for different methods. The integrals (23) over the 5th period are computed with 50 time steps over a period. ($\Delta t = 437s$). Measuring in this norm the differences between the techniques become more apparent. The techniques with smallest errors are the Crank-Nicolson method and the symmetrical splitting technique. These are also the 2nd order in time methods. The effect of making the splitting operators symmetric over a double step is illustrated in the sequence of figures 4, 5 and 6. We note that areas with too large net flow cancel areas with too small net flow when we make the operator symmetric and 2nd order over a double step.

Parameters	Values	Parameters	Values
g	$9.81ms^{-2}$	l	$5.236 \times 10^{-6}m^{-1}$
f	$1.3 \times 10^{-4}s^{-1}$	k	$6.283 \times 10^{-6}m^{-1}$
H	$100m$	κ	$8.179 \times 10^{-6}m^{-1}$
W	$6 \times 10^{5}m$	ω	$2.873 \times 10^{-4}s^{-1}$
L	$3 \times 10^{6}m$	$\frac{2\pi}{\omega}$	$21872s$
n_x	6	$\frac{\partial\omega}{\partial k}$	$21.46ms^{-1}$
n_y	1	$\sqrt{gH}$	$31.32ms^{-1}$
η_0	0.5m		

Table 1. Physical parameters.

	Time steps (s)						
Method	73	109	219	437	875	1458	2187
Forward-backward	0.061	0.067	0.085	0.154	*	*	*
Crank-Nicolson	0.052	0.054	0.066	0.110	0.28	0.72	1.58
Backhaus-Wais	0.051	0.053	0.063	0.101	0.25	0.62	1.41
GC	0.052	0.054	0.063	0.097	0.23	0.51	1.15
CG	0.053	0.056	0.069	0.107	0.25	0.58	1.27
CGGC	0.052	0.053	0.066	0.108	0.28	0.71	1.76
$G_{xy}C$	0.052	0.054	0.064	0.094	0.22	0.50	1.20
CG_{xy}	0.053	0.056	0.068	0.107	0.25	0.59	1.31
$CG_{xy}G_{xy}C$	0.051	0.053	0.064	0.105	0.27	0.71	1.70
G_yG_xC	0.053	0.058	0.079	0.141	0.32	0.66	1.32
CG_xG_y	0.060	0.067	0.095	0.164	0.35	0.78	1.58
$CG_xG_yG_yG_xC$	0.051	0.053	0.063	0.103	0.27	0.74	1.78

Table 2. Maximum errors in approximations to η (m). (* = instability)

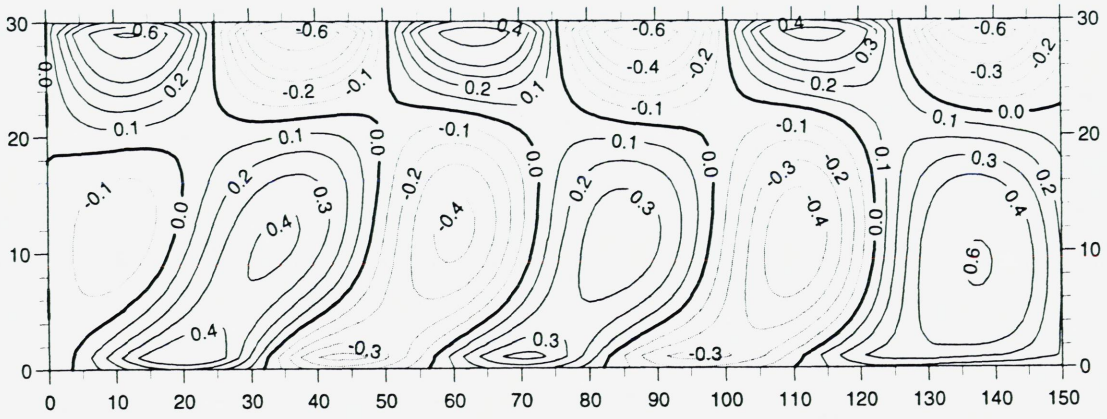

Fig. 2 Errors in the approximations to $\overline{U}$ for the forward-backward method. Max. error = $0.832 m^2 s^{-1}$.

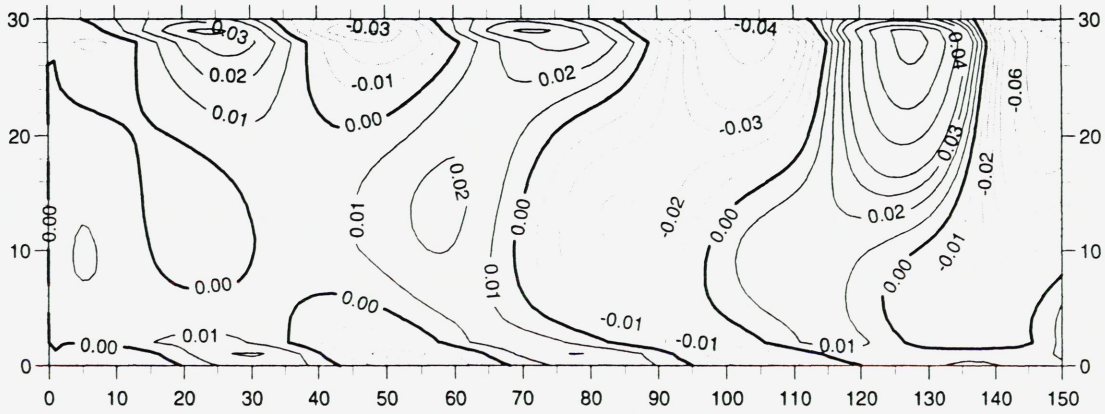

Fig. 3 Errors in the approximations to $\overline{U}$ for the Crank-Nicolson method. Max. error = $0.106 m^2 s^{-1}$.

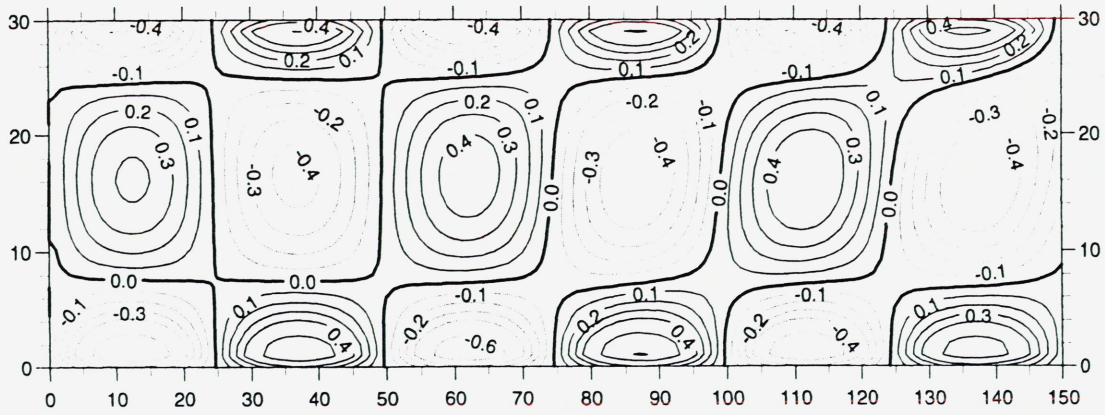

Fig. 4 Errors in the approximations to $\overline{U}$ for the method with propagation matrix $G_y G_x C$. Max. error = $0.808 m^2 s^{-1}$.

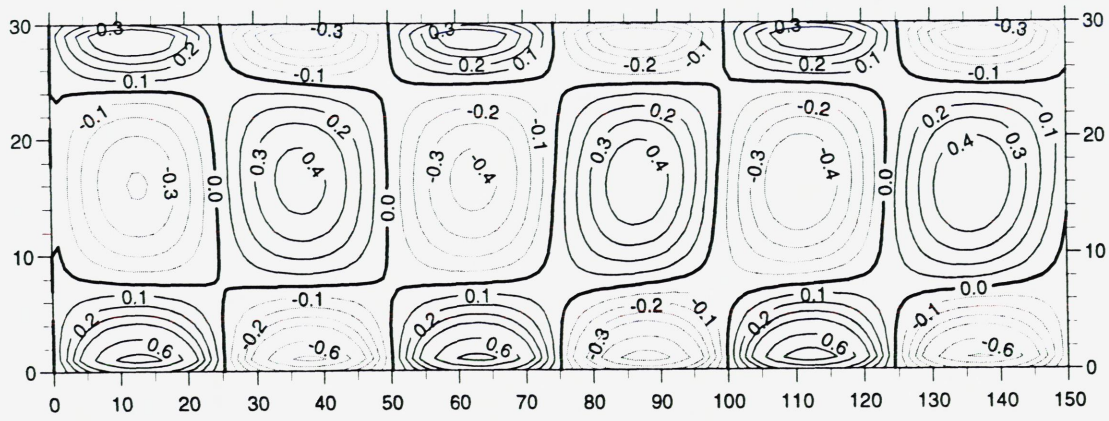

Fig. 5 Errors in the approximations to $\overline{U}$ for the method with propagation matrix CG_xG_y. Max. error = $0.912m^2s^{-1}$.

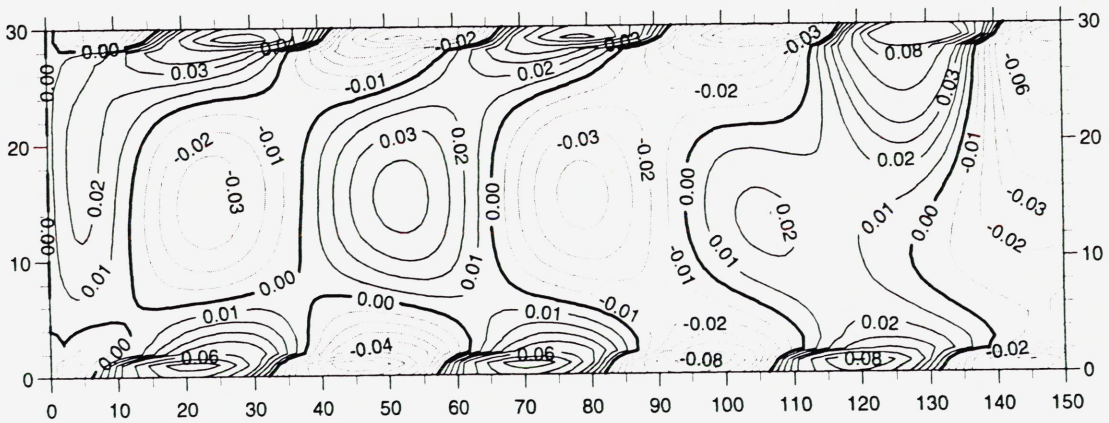

Fig. 6 Errors in the approximations to $\overline{U}$ for the method with propagation matrix $CG_xG_yG_yG_xC$. Max. error = $0.165m^2s^{-1}$.

4 M_2 tide in the North Sea.

In order to study the quality of the time stepping techniques for a more realistic case, models for approximating the circulation and water level of the North Sea are implemented. In Fig. 7 the bottom topography is given. The resolution is $20km$. Estimates of the M_2-tidal values are added to monthly climatological values and applied as initial and boundary values, see Martinsen et al. [11]. The boundary values in a 10 cell wide FRS-zone are updated every model time step. The CFL-criterion for the forward-backward method is $75.8s$. In Fig. 8 the water level after one M_2-cycle (12.42 hours) is approximated with the Crank-Nicolson

method and $\Delta t = 18.6s$. For small time steps the spatial errors dominate and because the spatial discretizations are the same for all time stepping procedures, the differences in maximum water levels after one M_2-cycle are less than $0.01m$ for all the suggested techniques. The total errors in the approximations presented in Fig. 8 are uncertain. However, the time discretization errors are considered to be small and results produced by the Crank-Nicolson method and $\Delta t = 18.6s$ will therefore be used as a reference when discussing time discretization errors for the suggested techniques for longer time steps.

The fields vary rapidly in space and time and the pointwise errors may therefore be very large. We therefore prefer to study the errors in M_2-period integrated values of η and $\underline{U}/H$ which are denoted as $\overline{\eta}$ and $\overline{(\underline{U}/H)}$, see (23). We also measure the the average absolute errors in the fields over all sea cells

$$\overline{\eta}_a = \frac{1}{\text{number of sea cells}} \sum_{\text{all sea cells}} |\overline{\eta} - \overline{\eta}_{exact}|$$

where $\overline{\eta}_{exact}$ are the results as computed by Crank-Nicolson and $\Delta t = 18.6s$. Correspondingly also $\overline{(\underline{U}/H)}_a$ is computed. In Table 3 values of $\overline{\eta}_a$ for different time stepping techniques are presented and in Table 4 values of $\overline{(\underline{U}/H)}_a$ for different time stepping techniques are given. The results of tables 3 and 4 indicate that we may apply considerably longer time steps than the CFL-criterion and still get acceptable results for the average flow. We note that to split the Coriolis terms from the gravity terms to reduce the computational complexity does not decrease the quality significantly and this splitting does not cause any stability problems. The spatial splitting techniques with propagation matrices $G_{xy}C$ and $CG_{xy}G_{xy}C$ become unstable for the time steps applied in this experiment that are longer than the CFL-criterion. However, by making the spatial splitting symmetric over a double step, we get acceptable results for time steps that are 10 times longer than the CFL criterion. (60 steps per M_2 cycle.) For even longer time steps also the symmetrical splitting technique $CG_{yx}G_{xy}C$ will, however, become unstable. In order to illustrate the effect of alternating the order in which the operator is split spatially, η after one M_2 cycle as computed by the Crank-Nicolson method and $\Delta t = 745.2$s is plotted in Fig. 9. Corresponding results for the spatial splitting techniques $CG_{xy}G_{xy}C$ and $CG_{yx}G_{xy}C$ are presented in figures 10 and 11. Comparing figures 8 and 9 we find differences in water levels in many areas. The largest difference is 0.95m and located south-east of England where we also find large spatial gradients. The main features of the tide are, however, still present and the positions and strengths of the maxima/minima are similar. From Fig. 10 we note that performing an unsymmetric spatial split introduces many 1-D structures in deeper waters, along the Norwegian coast and in Skagerrak. These 1-D structures are removed when the operators are symmetrized over a

double step as we see from Fig. 11. The time discretization errors are now similar to the corresponding errors for the Crank-Nicolson method.

The results for spatial splitting techniques with propagation matrices G_yG_xC and especially $CG_xG_yG_yG_xC$ are even more promising, see figures 12 and 13. The methods seem unconditionally stable. This was a surprise because all spatial splitting techniques suggested here are according to a von Neumann stability analysis stable for free waves, but it seems that the techniques based on splitting the differential equations have much better stability properties for realistic cases with varying topography.

Weare [13] studied the errors arising from irregular boundaries in ADI solutions of the shallow water equations. The ADI method analysed is similar to our method G_{xy}. Our results indicate that to regard the problem in substeps as 1-D problems may have a significant effect on the stability properties.

	Time steps (s)					
Method	18.6	74.5	372.6	745.2	1117.9	1490.5
Forward-backward	0.003	0.002	*	*	*	*
Crank-Nicolson	'exact'	0.007	0.023	0.030	0.032	0.033
GC	0.001	0.005	0.019	0.030	0.037	0.043
CGGC	0.001	0.007	0.021	0.029	0.034	0.039
$G_{xy}C$	0.001	0.006	*	*	*	*
$CG_{xy}G_{xy}C$	0.002	0.013	*	*	*	*
$CG_{yx}G_{xy}C$	0.001	0.013	0.030	0.033	*	*
G_yG_xC	0.004	0.013	0.051	0.085	0.110	0.134
$CG_xG_yG_yG_xC$	0.001	0.005	0.023	0.033	0.047	0.066

Table 3. Values of $\overline{\eta}_a$ (m) over the 5th M_2 cycle. (* = instability)

	Time steps (s)					
Method	18.6	74.5	372.6	745.2	1117.9	1490.5
Forward-backward	0.002	0.002	*	*	*	*
Crank-Nicolson	'exact'	0.005	0.020	0.031	0.039	0.044
GC	0.001	0.007	0.030	0.049	0.063	0.073
CGGC	0.001	0.007	0.030	0.048	0.061	0.071
$G_{xy}C$	0.001	0.007	*	*	*	*
$CG_{xy}G_{xy}C$	0.002	0.011	*	*	*	*
$CG_{yx}G_{xy}C$	0.001	0.011	0.036	0.052	*	*
G_yG_xC	0.002	0.006	0.030	0.051	0.067	0.080
$CG_xG_yG_yG_xC$	0.001	0.007	0.039	0.070	0.090	0.109

Table 4. Values of $\overline{(\underline{U}/H)}_a$ (ms^{-1}) over the 5th M_2 cycle. (* = instability)

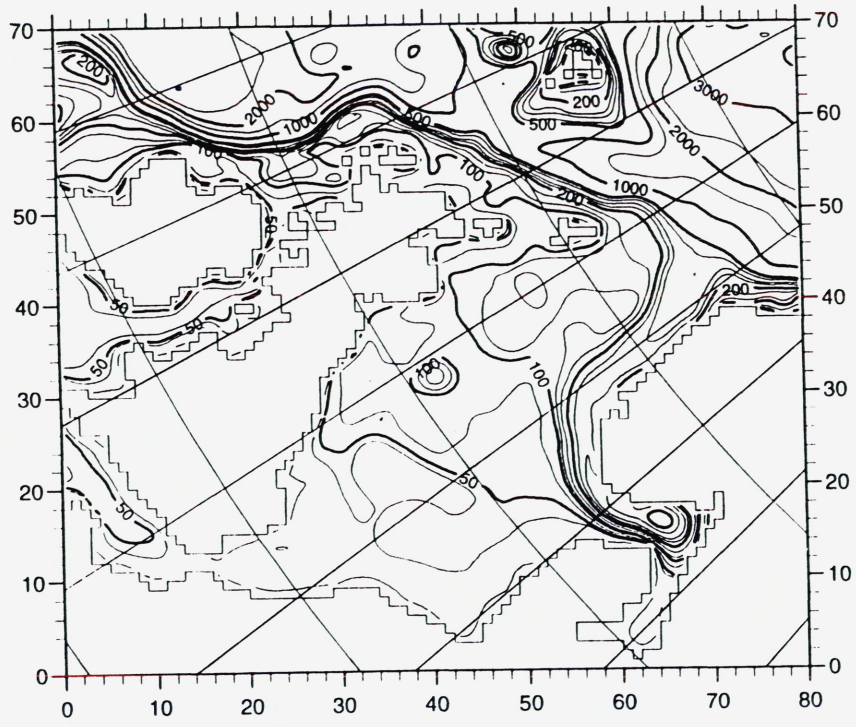

Fig. 7 Bottom topography of the North Sea.

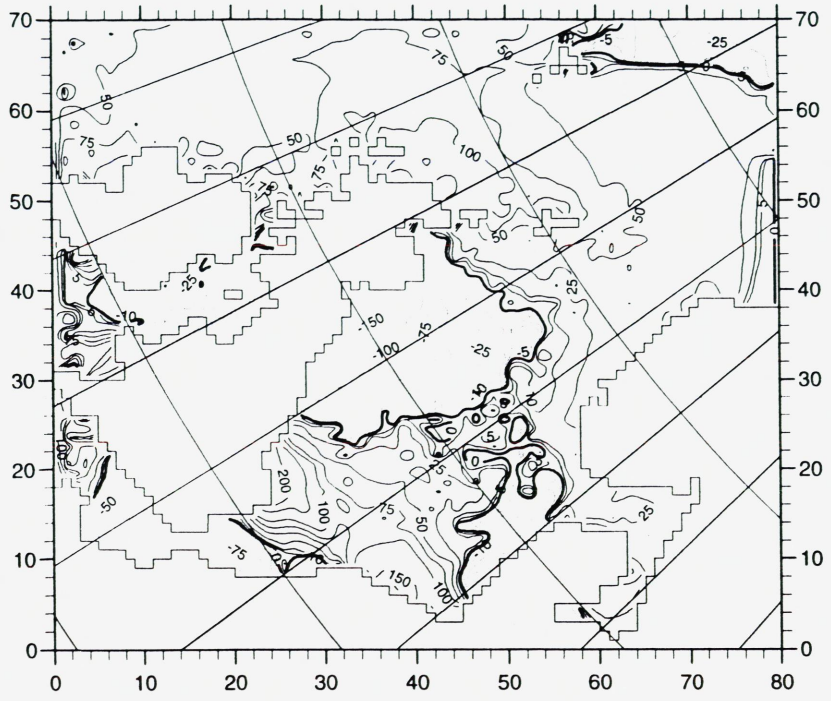

Fig. 8 η after 1 M_2-cycle produced by the Crank-Nicolson method and $\Delta t = 18.6s$. Max. $|\eta| = 3.33m$.

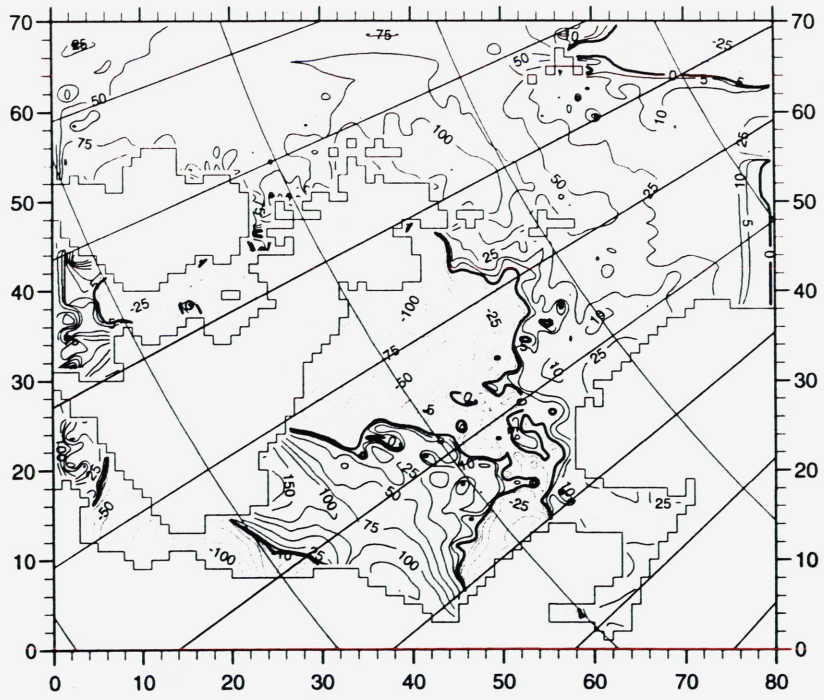

Fig. 9 η after 1 M_2-cycle produced by the Crank-Nicolson method and $\Delta t = 745.2s$. Max. $|\eta| = 3.23m$.

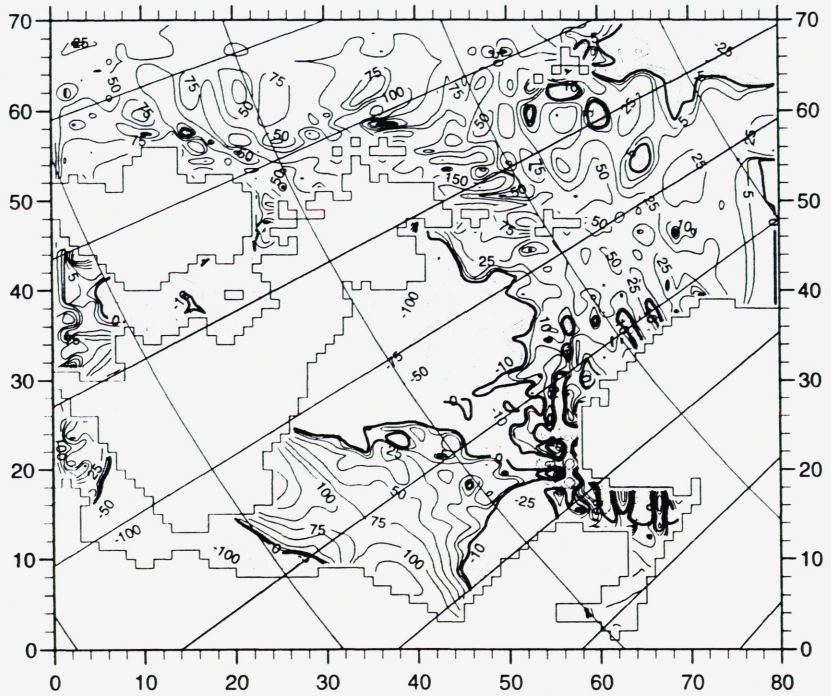

Fig. 10 η after 1 M_2-cycle produced by the $CG_{xy}G_{xy}C$ method and $\Delta t = 745.2s$. Max. $|\eta| = 7.33m$.

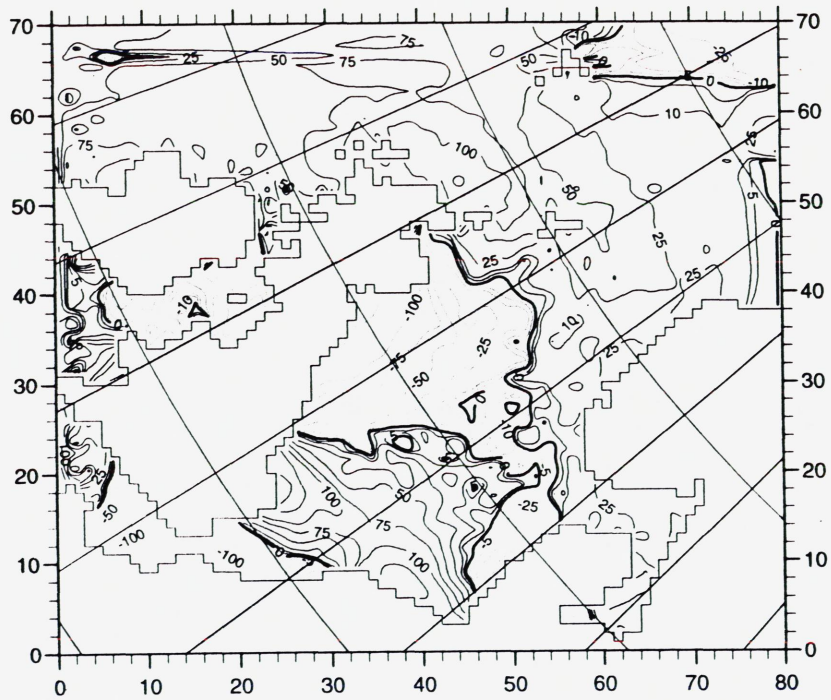

Fig. 11 η after 1 M_2-cycle produced by the $CG_{yx}G_{xy}C$ method and $\Delta t = 745.2s$. Max. $|\eta| = 3.23m$.

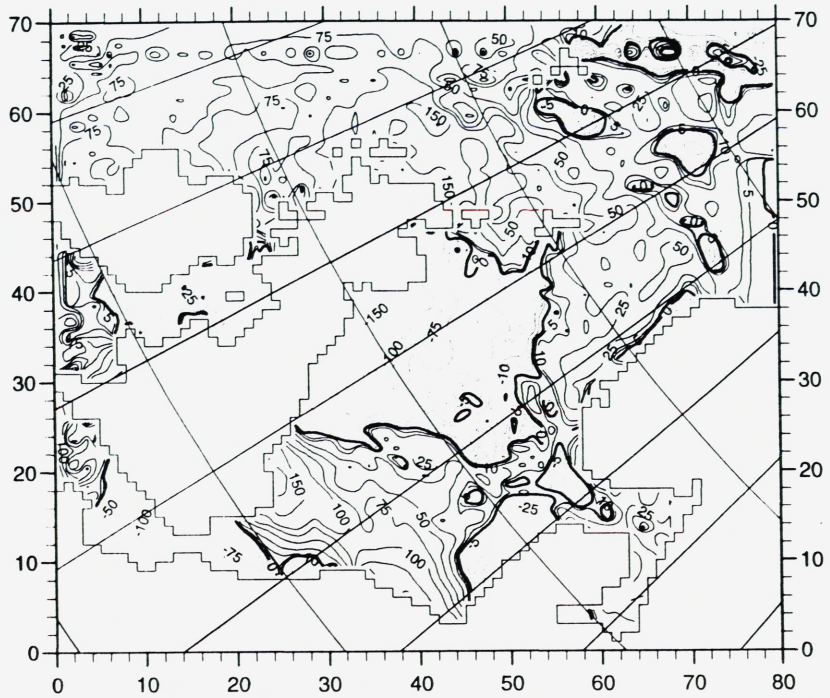

Fig. 12 η after 1 M_2-cycle produced by the G_yG_xC method and $\Delta t = 745.2s$. Max. $|\eta| = 3.23m$.

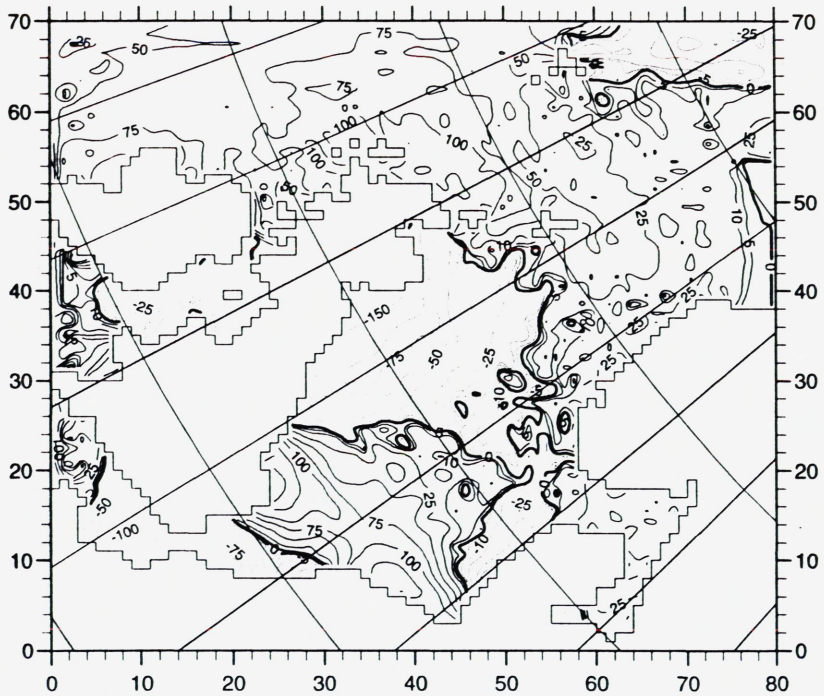

Fig. 13 η after 1 M_2-cycle produced by the $CG_xG_yG_yG_xC$ method and $\Delta t = 745.2s$. Max. $|\eta| = 3.23m$.

5 Conclusions.

When applying implicit methods in free surface ocean models, the CFL-criterion is avoided, but large linear systems of equations with large bandwidths may have to be solved at each time step. The question raised in this paper is whether it is possible to split the original problem into a series of subproblems in such a way that: a) The computational complexity of a subproblem will be at most to solve a three diagonal system of equations and b) the qualities of the model results are acceptable when we use time steps substantially larger than the CFL criterion for explicit methods.

We have approached the answer to this question in two stages. The differential equations are first split into two subsystems, one including the Coriolis terms only and one with the gravity terms and the equation of continuity. Then the last subsystem is split spatially, either by splitting the gravity difference equations or by splitting the corresponding differential equations before discretization.

The results from our experiments indicate that the differential equations may be split into our two subsystems without any significant loss of accuracy. At least this is the case when the operations are symmetrized over a double step. Such a split reduces the computational complexity considerably, but we still have to solve linear equations with large bandwidths at each time step.

All spatial splitting techniques suggested are for free waves and constant depth unconditionally stable. For the case with varying topography and non-straight coasts the techniques based on splitting the gravity differential equations spatially proves to have much better stability properties than the technique based on splitting the difference equations. The former techniques seem to be unconditionally stable, but a study of the eigenvalues of the corresponding propagation matrices remains to be done. Taking the computational complexity and the apparent robustness into account, we regard the symmetrized splitting technique based on splitting the differential equations spatially to be a very attractive alternative to the Crank-Nicolson method applied to the coupled system of equations.

The experiments described in this paper are performed without any horizontal eddy diffusion. Introducing diffusion smooths the numerical approximations and the results become even more in favor of symmetrical spatial splitting techniques.

Nonlinear terms or advection of momentum are avoided in this study. The CFL-criterion time step invoked when introducing these terms and applying explicit methods is typically much larger than the corresponding criterion for free surface gravity waves. It is therefore hoped that these terms may be treated in separate fractional steps with explicit methods.

References

[1] J.O. Backhaus. A semi-implicit scheme for the shallow water equations for applications to shelf sea modeling. *Contin. Shelf Res.* **2**,243 (1983).

[2] J.O. Backhaus. A three-dimensional model for the simulation of shelf sea dynamics. *Dt. Hydrogr. Z.* **38**,165 (1985).

[3] J.-M. Beckers and E. Deleersnijder. Stability of a FBTCS scheme applied to the propagation of shallow water inertia-gravity waves on various space grids. *J.Comput.Phys.* **108**,95 (1993).

[4] V. Casulli. Semi-implicit Finite Difference Methods for the Two-Dimensional Shallow Water Equations. *J.Comput.Phys.* **86**,56 (1990).

[5] J. Crank and P. Nicolson. A practical method for numerical evaluation of solutions of partial differential equations of the heat- conduction type. *Proc. Cambridge. Philos. Soc.* **43**,50 (1947).

[6] J.K. Dukowicz and A.S. Dvinsky. Approximate Factorization as a High Order Splitting for the Implicit Incompressible Flow Equations. *J.Comput.Phys.* **102**, 336 (1992).

[7] A.E. Gill. *Atmosphere-Ocean Dynamics.* (Academic Press, 1982).

[8] G.J. Haltiner and R.T. Williams. *Numerical prediction and dynamic meteorology.* (John Wiley, 1980).

[9] W.H. Hundsdorfer and J.G. Verwer. Stability and Convergence of the Peaceman-Rachford ADI Method for Initial-Boundary value Problems. *Math.Comp.* **53**, 81 (1989).

[10] E.A. Martinsen and H. Engedahl. Implementation and testing of a lateral boundary scheme as an open boundary condition in a barotropic ocean model. *Coastal Engineering.* **11**,603 (1987).

[11] E.A. Martinsen, H. Engedahl, G. Ottersen, B. Ådlandsvik, H. Loeng, and B. Balino. *Climatological and hydrographical data for hindcast of ocean currents.* The Norwegian Meteorological Institute, Technical Report Tech. Rep 100, 1992.

[12] G. Strang. On the construction and comparison of different schemes. *SIAM J.Numer.Anal.* **5**,506 (1968).

[13] T.J. Weare. Errors arising from irregular boundaries in ADI solutions of the shallow-water equations. *Int.J.Numer.Meth.Eng.* **14**,921 (1979).

[14] T. Weiyan. *Shallow water hydrodynamics.* (Elsevier Oceanography Series, 1992).

Depotbiblioteket
78sd 20 245